Original Article
Intravoxel incoherent motion MR imaging in breast cancer: quantitative analysis for characterizing lesions

Naier Lin[1], Junyan Chen[2], Jia Hua[3], Jinhua Zhao[1], Jun Zhao[4], Jinsong Lu[5]

[1]Department of Nuclear Medicine, Shanghai General Hospital, School of Medicine, Shanghai Jiao Tong University, Shanghai, P. R. China; [2]Philips Healthcare, Shanghai, P. R. China; [3]Department of Radiology, [5]Comprehensive Breast Health Center, Renji Hospital, School of Medicine, Shanghai Jiao Tong University, Shanghai, P. R. China; [4]School of Biomedical Engineering, Shanghai Jiao Tong University, Shanghai, P. R. China

Abstract: Objectives: We compared the monoexponential model diffusion weight imaging (DWI) and intravoxel incoherent motion DWI (IVIM-DWI) parameters for characterizing different subtypes and grades of breast cancer lesions. Methods: We analyzed 93 patients (51 with breast cancers and 47 with benign lesions) using monoexponential (b=0.800 s/mm^2) and biexponential analysis (b=0-800 s/mm^2) and 3.0T MRI. We compared the apparent diffusion coefficient (ADC), true diffusion coefficient (D), perfusion fraction (f) and pseudo-diffusion coefficient (D*) in different subtypes and grades of cancers. We used receiver operating characteristics (ROC) to identify the best cutoff for differentiation between lesions. Results: All data showed good fit (R^2>0.90). The D value was significantly lower than ADC in all the lesions except cysts (P<0.05). ADC, D and D* in malignant tumors were significantly lower than those in benign ones (P<0.001 for ADC and D; 0.002 for D*). The f value was higher than that of benign lesions (P<0.001). D showed higher accuracy than ADC in differentiating malignancy from benign lesions (AUC=0.945 for D; 0.931 for ADC), or ductal carcinoma in situ (DCIS) from invasive ductal carcinoma (IDC) (AUC=0.791 for D; 0.675 for ADC). Furthermore, the D value was significantly lower in high grade IDC (TNM III) than in low grade IDC (TNM I+II) (P=0.006), while no other parameters showed a difference between varied grades of IDC (P>0.05). Conclusions: IVIM provides quantitative measurement of cellularity and vascularity for characterizing breast lesions. In particular, D shows good potential for grading breast cancer.

Keywords: Intravoxel incoherent motion, diffusion-weighted imaging, biexponential signal attenuation, apparent diffusion coefficient, breast cancer

Introduction

In recent years, the incidence rate of breast cancer has risen sharply in China and it has become a large threat to women's lives. Identification breast cancer at an early stage can facilitate early treatment and is a particularly useful for breast-observing treatment [1]. Biopsy is the standard technique for diagnosing pre-operative breast cancer; however, its value may be limited by the potential risks for sampling error [2].

During the last few years, with the development of functional MRI technology, diffusion weighted MRI (DWI-MRI) has evolved into a promising tool to increase the specificity of breast lesion diagnosis [3]. The apparent diffusion coefficient (ADC) derived from DWI is significantly affected by motion of water molecules at a microscopic level, and thus can provide information about tissue microenvironment [4-6]. However, given the relatively high vascularity and cellularity of breast cancer, conventional DWI based on the monoexponential model is not precise enough to characterize tissue components. Intravoxel incoherent motion (IVIM), a more sophisticated approach first proposed by Le Bihan et al. [7], gives rise to quantitatively biexponential assessment of tissue perfusion and diffusion parameters with multi b values. Due to its potential advantages, there is a growing interest in applying IVIM models to body organs, such as the prostate [8], liver [9, 10], and pancreas [11], and to the head and neck [12, 13]. Although a few IVIM studies in the breast [14-17] have demonstrated its feasibility

Table 1. Characteristics of lesions in this study

Benign lesions (N=47)		Malignant lesions (N=51)	
Fibroadenoma (FA)	22	DCIS	8
Intraductal papilloma (IDP)	6	Low grade IDC (TNM I+II)	25
Cyst	11	High grade IDC (TNM III)	14
Mastitis	3	Invasive lobular carcinoma	2
Fibrocystic disease	3	Paget's	2
Sclerosing adenosis	2		

and 31 benign lesions), needle biopsy specimens from 8 lesions (3 malignant lesions and 5FAs), and breast contrast-enhanced dynamic MRI in 11 cysts. Two pathologists (one doctor with 5 years' experience, and one with more than 10 years' experience) analyzed the specimens and identified the histological grade of tumors according to the TNM system.

in differentiating cancers from benign lesions, there has been little research on its value in distinguishing different histologic stages of breast cancer. Therefore, we hypothesize that this diffusion model could enhance characterization of breast tissue and be used as a significant predictor of histopathologic stage of breast lesions.

The purpose of our study is to 1) compare biexponential and monoexponential DWI parameters in a cohort of breast lesions and estimate the diagnostic ability of IVIM DWI at 3.0T MRI; and 2) research the IVIM parameters in different subtypes of breast lesions and compare the parameters in different histological grades of breast cancer.

Materials and methods

Patients

The studies were approved by ethics committee of Renji Hospital affiliated with the Medical School at Shanghai Jiaotong University. All patients signed the informed consent form. Ninety-three patients (females with a mean age of 48 years, ranging from 17 to 77 years) with a total of 98 breast lesions diagnosed from January 3, 2014 to January 1, 2016 were included in this study. All of the subjects had either prior signs or a diagnosis of breast lesions (via mammography or ultrasound). Lesions were excluded from our analysis if they were smaller than 6 mm, or if the MR images had susceptibility artifacts or poor fat suppression. All the 98 cases are shown in **Table 1**. Within the 51 malignant lesions group, one patient had both a DCIS lesion and an IDC lesion, one patient had both an IDC lesion and an ILC lesion, two patients had a Paget's lesion and an IDC lesion, and another one patient had two IDC lesions on one side of her breast. The final diagnosis was established on the basis of histopathological examination of surgical specimens from 79 lesions (48 malignant lesions

Imaging

MR imaging was performed using a 3.0T MR imager (Achieva 3.0 T, Philips Healthcare, Best, Netherlands) equipped with a standard 4-channel SENSE breast coil in a prone position.

Diffusion-weighted imaging

Patients underwent diffusion-weighted axial imaging using the spin-echo-type single-shot echo planer imaging (EPI) with SPAIR before administration of Gd-DTPA. The monoexponential DWI had weighting factors of b 0, 600 s/mm^2 (TR/TE: 5363/450 ms; FOV: 320×330 mm^2; acquisition matrix: 200×196; slice: 36; thickness/gap: 4/1 mm, total scan time: 02:05 min). The IVIM-DWI had weighting factors of b 0, 50, 100, 150, 200, 500, 800 s/mm^2 (TR/TE: 2000/69 ms; FOV: 170/170/72 mm^2; vox size: 2×1.3 mm; acquisition matrix 84×131; thickness/gap: 4/0.8 mm, total scan time: 03:22 min). The IVIM DWI scan did not achieve full breast coverage, but the lesion of interest was chosen.

Contrast-enhanced imaging

Axial T1-weighted high-resolution isotopic volume examination (THRIVE) 3D gradient-echo sequence with active fat suppression was performed before and 43 seconds after contrast injection (TR/TE: 4.7 ms/2.3 ms; flip angle: 10; slice thickness/gap: 1 mm/0; Fov: 320/320/150 mm), matrix: 400*320, the temporal resolution was 60 s, total scan time: 6 min). A gadolinium-based agent Gd-DTPA (Injection Dimeglumine gadopentetate, Magnevist; Bayer Healthcare, Berlin, Germany) was intravenously injected at a dose of 0.1 mmol/kg with a high pressure injector at the rate of 1.5 ml/s. The contrast injection was follow by a 20 ml saline flush.

Table 2. Summary of Groups (Mean ± SD) from mono-exponential and bi-exponential analysis in different pathological breast lesion

|	ADC (*10^{-3} mm²/s)	D (*10^{-3} mm²/s)	f (%)	D*(*10^{-3} mm²/s)
Benign	1.478 ± 0.252	1.398 ± 0.295	6.402 ± 3.631	126.044 ± 40.920
Malignant	1.087 ± 0.126	0.933 ± 0.129	10.225 ± 2.764	101.203 ± 29.015
p	0.000	0.000	0.000	0.002
IDC	1.061 ± 0.117	0.903 ± 0.116	10.693 ± 2.870	101.029 ± 29.065
DCIS	1.164 ± 0.146	1.061 ± 0.163	9.354 ± 3.364	102.335 ± 34.720
p	0.017	0.013	0.084	0.932
High Grade IDC	1.026 ± 0.111	0.857 ± 0.101	11.718 ± 2.791	98.745 ± 31.299
Low Grade IDC	1.081 ± 0.119	0.928 ± 0.117	10.120 ± 2.805	102.308 ± 28.322
P	0.208	0.006	0.074	0.725
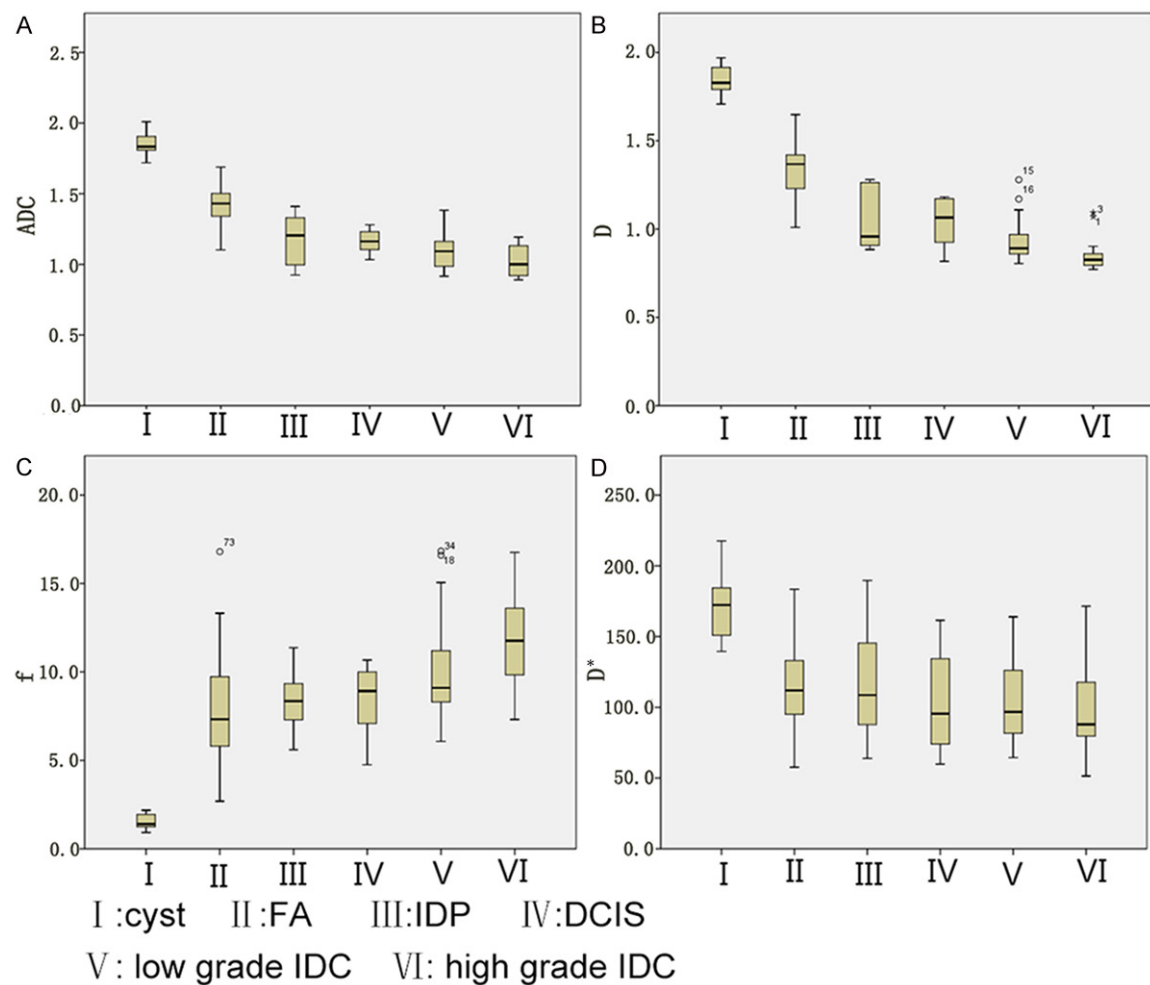
Figure 1. Specific range of ADC (A), D (B), f (C), D* (D) values corresponding to different tissue cellularity and vascularity. The higher ADC value than D in most of breast lesions indicating an obvious IVIM effect. Higher ADC, D, D* values and a lower f value were found in benign lesions than that of malignant ones.

Image processing and analysis

All the MR images were transferred to computer workstation (Extended Workspace, Philips Healthcare) for analysis. Lesions with hyperintensity on the post-contrast images were used as a guide for region of interest (ROI) placement. Two radiologists (one with more than 10
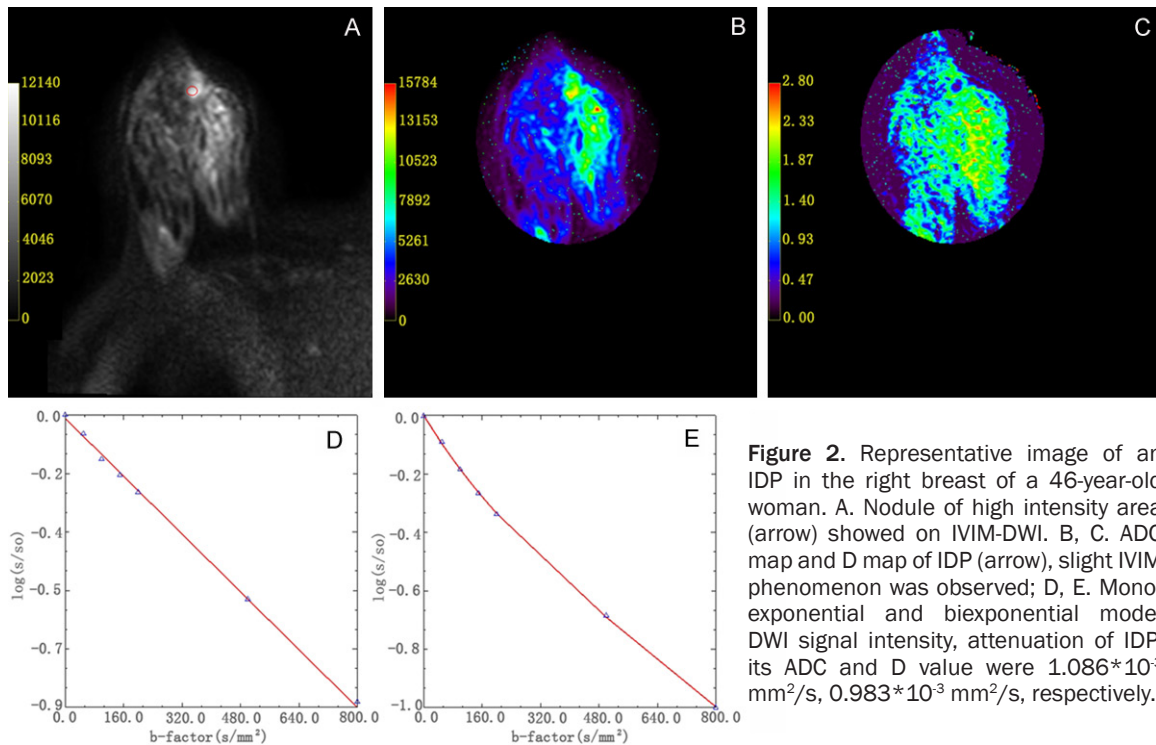
Figure 2. Representative image of an IDP in the right breast of a 46-year-old woman. A. Nodule of high intensity area (arrow) showed on IVIM-DWI. B, C. ADC map and D map of IDP (arrow), slight IVIM phenomenon was observed; D, E. Mono-exponential and biexponential model DWI signal intensity, attenuation of IDP, its ADC and D value were $1.086*10^{-3}$ mm^2/s, $0.983*10^{-3}$ mm^2/s, respectively.

years of experience in breast MRI diagnosis, another with 5 years of experience) were blinded to the lesion histology. The ADC map was generated with monoexponential decay model, and a monoexponential model was expressed using the following equation:

$$Sb/S0 = exp\,(-b\,ADC) \qquad [1]$$

where S0 is the signal intensity in the pixel without the diffusion gradient. The IVIM DWI series was reconstructed into the D map, f map, and D* map with the biexponential model using a manufacturer supplied software (IVIM DWI Tool, Philips Healthcare). The biexponential model was expressed by the following equation:

$$S/S_0 = f \cdot exp\,(-b\,(D+D^*)) + (1-f) \cdot exp\,(-b\,D) \qquad [2]$$

where Sb is the signal intensity with diffusion weighted b, D is the true diffusion in the vox reflecting pure molecular diffusion, f is the fractional perfusion related to microcirculation, and D* is the pseudo-diffusion coefficient representing perfusion-related diffusion or incoherent microcirculation. IVIM fitting curves were generated by substituting the estimated values of D*, f, and D into Equation [2].

In this study, we also calculated the goodness of fit (R^2) pixel by pixel for all the images. The goodness of fit was assessed using the following equation:

$$R^2 = 1 - SSE/SS_{total} \qquad [3]$$

where SSE is the sum of squared errors between the data and the fitting curves, and SS_{total} is the sum of the squared difference between the data and the mean of all data values. R^2 of data collected in this study were all above 0.90.

The ROI was manually drawn by a radiologist who specializes in breast cancer. For each patient, lesions were identified on axial DCE images and the slice that contained the maximum diameter of lesions was marked. Then the ROI on the DW images were drawn to match the location on the DCE MRI, with each ROI encompassing as much of the enhancing abnormality as possible. The mean ROI area in this study was 67 mm^2 (range from 18-314 mm^2). The ROI was placed 3 separate times for each of the lesions by two observers who were blinded to the lesion histology.

Statistical analysis

SPSS Statistics 19.0 software was used for the statistical analysis. The parameters are pre-

Table 3. Diagnostic efficiency of parameters in discrimination malignancy from benign lesions

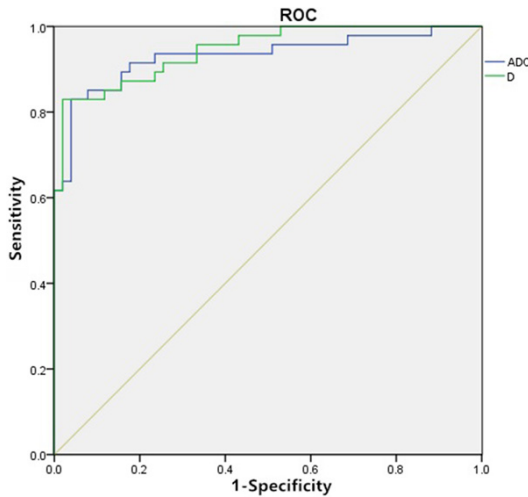|	AUC	95% CI	Cut off level	Sensitivity	Specificity
ADC	0.931	0.876-0.985	$1.203*10^{-3}$ mm^2/s	89.4%	84.3%
D	0.945	0.903-0.986	$1.096*10^{-3}$ mm^2/s	87.2%	84.3%
f	0.802	0713-0.891	$7.870*10^{-3}$ mm^2/s	86.3%	66.0%
D*	0.682	0575-0.788	$99.056*10^{-3}$ mm^2/s	70.2%	58.8%

Figure 3. ROC curve for the differentiation of benign and malignant lesions.

sented as the mean ± standard deviation. Interobserver agreement between the two observers during the measure of parameters was calculated using the intraclass correlation coefficient (ICC). A test of normal distribution for each group parameter was performed. A paired t-test was used to compare the ADC value and D value for different breast lesions. The Mann-Whitney U test was performed for further comparison of parameters between specific group pairs. P<0.05 was considered to be statistically significant.

Receiver operating characteristic (ROC) curve analyses were performed to assess the utility of ADC and IVIM parameters to detect malignancy from benign lesions, as well as DCIS from IDC. The area under the curve (AUC) of different parameters was compared to identify the diagnostic efficiency. Sensitivity and specificity were also calculated.

Results

There was excellent agreement in the ADC value, which had an ICC of 0.991, in the D value, which had an ICC of 0.896, and a relatively good agreement in the f value, which had an ICC of 0.861 and in the D* value, which had an ICC of 0.853.

D, f and D* from the biexponential fitting and ADC from the monoexponential fitting in pathological breast lesions are shown in **Table 2**. The ADC value is higher than D in all the lesions except in cysts (P<0.05), indicating an IVIM effect in these lesions. The D value in breast lesions is shown as the following: IDC<DCIS ≈ IDP (P>0.05)<FA< breast cyst. A higher ADC, D, and D* value and a lower f value were found in benign breast lesions compared with malignant lesions (**Figure 1**). All parameters were significantly different between malignant and benign lesions (P<0.001) for ADC, D, f; *P*=0.002 for D*).

IDP **Figure 2** showed the lowest ADC and D value among the benign lesions. There was no significant difference in any of the parameters between DCIS and IDP (P=0.796 for ADC; P=0.519 for D; P=0.846 for f; and P=0.519 for D*).

Table 3 and **Figure 3** show results of the ROC analysis for ADC, D, f and D* values in determining malignancy. We found that D had the best diagnostic efficacy (AUC=0.945), which was slightly higher than that of ADC (AUC=0.931). Using the cutoff level ≤1.096 10^{-3} mm^2/s for D and ≤1.096×10^{-3} mm^2/s for ADC, they had the same specificity (84.3%).

In the group DCIS *vs.* IDC, the mean value of D and ADC in IDC (1.061×10^{-3} mm^2/s for ADC; 0.903×10^{-3} mm^2/s for D) were significantly smaller than that of DCIS **Figure 4** (1.164×10^{-3} mm^2/s for ADC, P=0.017; 1.061×10^{-3} mm^2/s for D, P=0.013).

Table 4 show the ROC for detecting IDC from DCIS. D was found to be a better predictor than any of the other three parameters (AUC=0.791 for D). Using a cutoff ≤0.850×10^{-3} mm^2/s for D, sensitivity and specificity were 81.8% and 71.4%, respectively.

In the low grade IDC vs. high grade IDC **Figure 5**, only D showed a significant difference (0.857 ± 0.101×10^{-3} mm^2/s for high grade IDC, 0.928
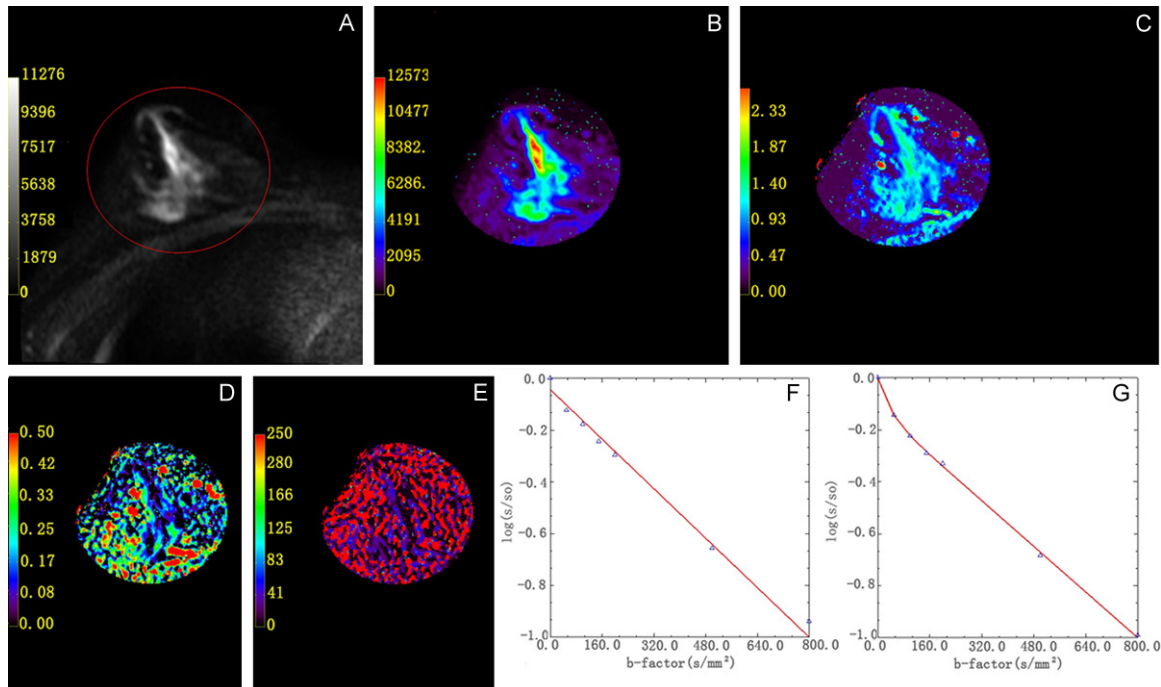
Figure 4. Representative image of a DCIS in the right breast of a 43-year-old woman. A. A duct-like area of high intensity in the breast showed on IVIM-DWI. B-E. ADC, D, and F maps of the lesion. F, G. The mono-exponential and bi-exponential model DWI attenuation of DCIS, an obvious IVIM phenomenon at the low b values were observed. ADC and D value of DCIS were 1.161×10^{-3} mm^2/s, 1.072×10^{-3} mm^2/s, respectively.

$\pm$ 0.117×10^{-3} mm^2/s for low grade IDC; P=0.006). Interestingly, in this study, there was no statistically difference in f and D* between the DCIS compared with IDC and low grade IDC compared with high grade IDC.

Discussion

3-T MRI is being used more frequently in clinical practice. The higher field strength and spatial resolution enable smaller lesions to be identified clearly using DWI [18]. However, with significant vascularity, the ADC model has an incomplete description of cancer samples and this severely limits quantitative specificity for lesion discrimination. Appreciation of the IVIM in the body is relatively new, since technologic advancements such as fast imaging techniques have only recently enabled multiple b-value DWIs to be acquired during routine examinations. Although some studies have reported the usefulness of IVIM imaging in other body regions, research on its use in breast tissue is limited. Based on a bi-compartmental model, which allows quantitative parameters from capillary perfusion and diffusivity to be derived, our study contributes to our understanding of the use of IVIM in diagnosis and grading of breast lesions.

This study presented an IVIM-based approach using 7 b values. Previous studies [18, 19] proposed that using more than 10 b values could strengthen the IVIM effect and a lower b (between 0 and 200 s/mm^2) used in IVIM could result in a more accurate perfusion parameter. However, taking the limited examination time into account, it is impossible to apply a large number of b values in the clinic, so we used 7 b values in the current study and most of them were not larger than 200 s/mm^2.

Among all breast lesions, only cysts fit a mono-exponential model of signal decay (D value was similar to ADC value, f fraction was very low). In most breast lesions, significantly lower D values compared with ADC values (P<0.05) were observed, indicating that a microperfusion effect contributed to the apparent diffusion. The box plots in **Figure 1** show the specific range of IVIM parameter values corresponding to different tissue cellularity and vascularity. In benign lesions, we found significantly higher ADC, D, D* and lower f fractions. However, this

Table 4. Diagnose efficiency of parameters in discriminating DCIS from IDC

	AUC	95% CI	Cut off level	Sensitivity	Specificity
ADC	0.675	0.497-0.853	$1.028*10^{-3}$ mm^2/s	72.7%	64.3%
D	0.791	0.635-0.947	$0850*10^{-3}$ mm^2/s	81.8%	71.4%

result did not agree with Tamura [15], who found no difference in any of the IVIM parameters between breast cancer and benign lesions. We suggest that this is due to the different choice of b-factors in IVIM imaging. In Tamura's study, higher b values (>800 s/mm^2) were used, and thus the IVIM effect of the malignant lesion that contributed to apparent diffusion was underestimated.

In this study, IDP was the most frequently encountered histological false-positive lesion with a lower D value than other benign lesions. In addition, there was no significant difference in any of the IVIM parameters between IDP and DCIS (P>0.05). This may result from the IDP pathologic features [20, 21], which arise from the segment of the interlobular or duct system at a deeper level. Its proliferative nature can result in high cellularity. However, taking the small IDP sample size (only 6) into account, further research with a larger sample size is needed to address the specific IVIM characteristics of IDP.

Previous studies show that faster signal decay is caused by both high vascularity (high f and D* value) and high cellularity (low D value) in breast cancer. Lee et al. found that the mean value of D* and f showed a significant correlation with microvessel density in cancer (P<0.001), while true diffusion did not (P=0.508), indicating that D is a better parameter than ADC for differentiating malignancy by avoiding vascular contributions [22]. In agreement with Lee, Liu found that the AUC of D was slightly better than that of ADC in differentiating between breast cancer and benign lesions [14]. Although the same trend was observed in our study, the specificity of the D value was lower than that found by Liu. This may due to our complex data set with a larger proportion of IDPs and DCISs, thus resulting in more overlap in D values.

For further comparison, we investigated the parameters in IDC and DCIS. IDC showed a marked lower D and ADC value than did DCIS, which is associated with increased cellular density and smaller extracellular volume fraction in IDC. AUC for D in identifying DCIS from IDC was much higher than that of ADC, suggesting that IVIM has good potential for early identification of noninvasive ductal carcinoma. Although a few reports [23, 24] have developed the relationship between ADC values and histological grade in breast tumors, these reports calculated ADC values based on the monoexponential DWI, which did not separately reflect tissue diffusivity and the micro-capillary perfusion effect. In this research, we found that there is no difference in ADC values in different grades of IDC, while true diffusion (D) of low grade IDC was significantly lower than that of high grade IDC. This reflects the stronger diagnostic value of D in predicting breast cancer risk compared with the ADC value. IVIM is more accurate in reflecting specific characteristics of tumor biology.

Angiogenesis is a necessary requirement for invasive cancer growth. Although many studies have demonstrated the usefulness of the microcapillary perfusion-sensitive parameters f and D* for disease characterization, in this study we found no significant difference in both f and D* in the DCIS vs. IDC and low grade IDC vs. high grade IDC groups. The weak diagnostic ability of the f and D* values are caused mainly by two factors. First, the slow enhancement in noninvasive ductal carcinoma - notably DCIS - was similar to that of benign lesions and breast parenchyma [25], so the perfusion fraction was less important than the diffusion fraction or cellularity for grading breast lesions. Second, in the IVIM model, D* and f may be an incomplete description of the tissue blood velocity or vascularity within breast lesions. Some researchers [18] have proposed that at low b values, some bulk flow effect can also result in the signal attenuation, although the intravoxel spin dephasing was mostly caused by the pseudo-random blood flow. Therefore, it is difficult to precisely distinguish fast tissue diffusion components in the IVIM model.

The measurement reproducibility of f and D* were not as good as that of ADC and D in the current study. A similar trend was reported in a recent study in liver by Andreou et al. [26], in
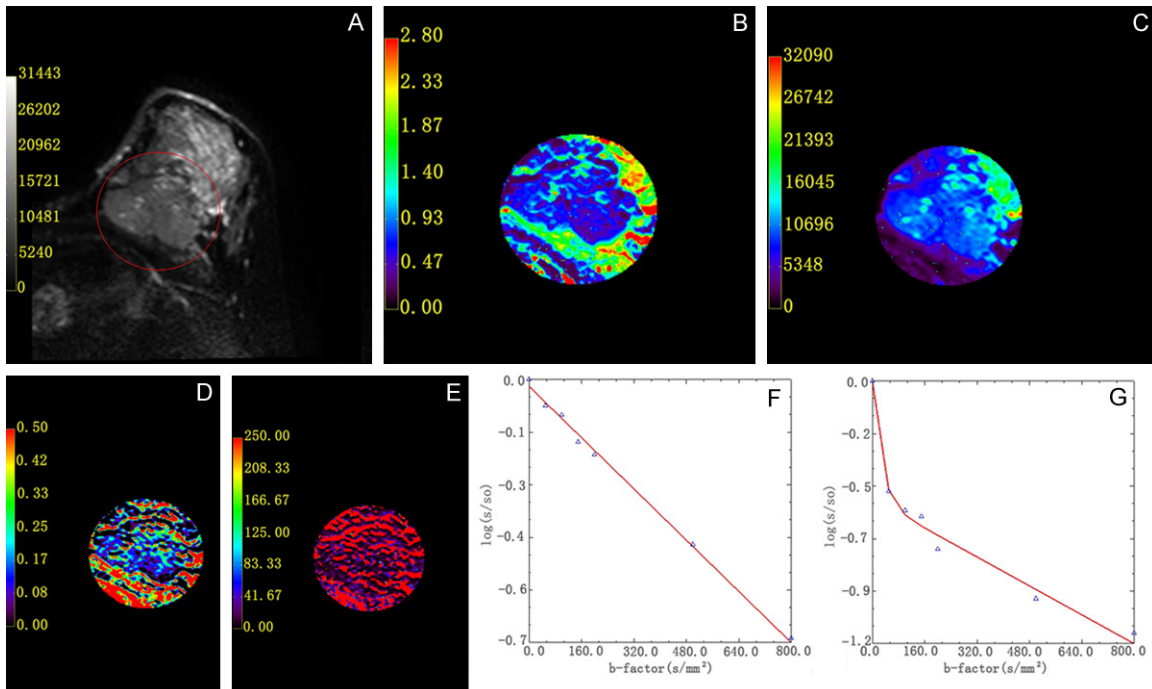
Figure 5. Representative image of a high grade IDC in the left breast of a 29 year-old woman. A. A high intensity clump in the left breast shows on IVIM-DWI. B-E. ADC, D, f, and D* maps for this cancer. F, G. monoexponential and biexponential model DWI signal intensity attenuation. The IVIM signal intensity decays quickly at low b and D values $(0.791×10^{-3}$ mm^2/s) and was significantly lower than the ADC value $(0.843×10^{-3}$ mm^2/s).

which relative poor reproducibility of f and D* were found particularly in metastases. However, to our knowledge, few studies to date have questioned the reproducibility of IVIM parameters that can reflect the observer errors and biological variations. Therefore, more test - retest reproducibility studies are needed to improve the level of confidence that can be ascribed to changes of f and D*in measurements when we applied this sophisticated mathematical model.

Our study had several limitations. First, we evaluated a limited number of patients with a small range of disease types. Thus, a larger sample size with a broader histological grade of breast lesions is necessary to support our results. Second, despite our attempts to minimize errors by manual placing of ROIs, there was still a bias in the measurement process. So, multiple planes (axial and sagittal imagines) are required to yield more accurate results.

In conclusion, as a potential imaging biomarker for disease characterization, IVIM DWI MRI, a radiation-free and media-free method, shows more promise than monoexponential DWI for identifying breast cancer and grading tumor risk by quantitatively assessing tissue perfusion and diffusion parameters with an increasing b value. Further research is needed to develop a suitable IVIM method (e.g. optimal choice of b) for clinical settings.

Disclosure of conflict of interest

None.

Address correspondence to: Jinhua Zhao, Department of Nuclear Medicine, Shanghai General Hospital, 100 Haining RD, Hongkou District, Shanghai, P. R. China. Tel: +86-15921888621; E-mail: zhaojinhua1963@126.com

References

[1] Croswell J and Owings J. Screening for breast cancer. Am Fam Physician 2016; 94: 143-144.
[2] Hes O, Michal M, Boudova L, Tregka V, Suvova B and Neprasova P. The peroperative biopsy-

-an overview of its problematical aspects from the pathologist's viewpoint. Rozhl Chir 2004; 83: 329-332.

[3] Partridge SC, Rahbar H, Murthy R, Chai X, Kurland BF, DeMartini WB and Lehman CD. Improved diagnostic accuracy of breast MRI through combined apparent diffusion coefficients and dynamic contrast-enhanced kinetics. Magn Reson Med 2011; 65: 1759-1767.

[4] Kamitani T, Matsuo Y, Yabuuchi H, Fujita N, Nagao M, Jinnouchi M, Yonezawa M, Yamasaki Y, Tokunaga E, Kubo M, Yamamoto H, Yoshiura T and Honda H. Correlations between apparent diffusion coefficient values and prognostic factors of breast cancer. Magn Reson Med Sci 2013; 12: 193-199.

[5] Woodhams R, Ramadan S, Stanwell P, Sakamoto S, Hata H, Ozaki M, Kan S and Inoue Y. Diffusion-weighted imaging of the breast: principles and clinical applications. Radiographics 2011; 31: 1059-1084.

[6] Hirano M, Satake H, Ishigaki S, Ikeda M, Kawai H and Naganawa S. Diffusion-weighted imaging of breast masses: comparison of diagnostic performance using various apparent diffusion coefficient parameters. AJR Am J Roentgenol 2012; 198: 717-722.

[7] Le Bihan D, Breton E, Lallemand D, Grenier P, Cabanis E and Laval-Jeantet M. MR imaging of intravoxel incoherent motions: application to diffusion and perfusion in neurologic disorders. Radiology 1986; 161: 401-407.

[8] Liu X, Peng W, Zhou L and Wang H. Biexponential apparent diffusion coefficients values in the prostate: comparison among normal tissue, prostate cancer, benign prostatic hyperplasia and prostatitis. Korean J Radiol 2013; 14: 222-232.

[9] Yamada I, Aung W, Himeno Y, Nakagawa T and Shibuya H. Diffusion coefficients in abdominal organs and hepatic lesions: evaluation with intravoxel incoherent motion echo-planar MR imaging. Radiology 1999; 210: 617-623.

[10] Patel J, Sigmund EE, Rusinek H, Oei M, Babb JS and Taouli B. Diagnosis of cirrhosis with intravoxel incoherent motion diffusion MRI and dynamic contrast-enhanced MRI alone and in combination: preliminary experience. J Magn Reson Imaging 2010; 31: 589-600.

[11] Concia M, Sprinkart AM, Penner AH, Brossart P, Gieseke J, Schild HH, Willinek WA and Murtz P. Diffusion-weighted magnetic resonance imaging of the pancreas: diagnostic benefit from an intravoxel incoherent motion model-based 3 b-value analysis. Invest Radiol 2014; 49: 93-100.

[12] Federau C, Maeder P, O'Brien K, Browaeys P, Meuli R and Hagmann P. Quantitative measurement of brain perfusion with intravoxel in-coherent motion MR imaging. Radiology 2012; 265: 874-881.

[13] Lai V, Li X, Lee VH, Lam KO, Chan Q and Khong PL. Intravoxel incoherent motion MR imaging: comparison of diffusion and perfusion characteristics between nasopharyngeal carcinoma and post-chemoradiation fibrosis. Eur Radiol 2013; 23: 2793-2801.

[14] Liu C, Liang C, Liu Z, Zhang S and Huang B. Intravoxel incoherent motion (IVIM) in evaluation of breast lesions: comparison with conventional DWI. Eur J Radiol 2013; 82: e782-789.

[15] Tamura T, Usui S, Murakami S, Arihiro K, Fujimoto T, Yamada T, Naito K and Akiyama M. Comparisons of multi b-value DWI signal analysis with pathological specimen of breast cancer. Magn Reson Med 2012; 68: 890-897.

[16] Sigmund EE, Cho GY, Kim S, Finn M, Moccaldi M, Jensen JH, Sodickson DK, Goldberg JD, Formenti S and Moy L. Intravoxel incoherent motion imaging of tumor microenvironment in locally advanced breast cancer. Magn Reson Med 2011; 65: 1437-1447.

[17] Tamura T, Usui S, Murakami S, Arihiro K, Akiyama Y, Naito K and Akiyama M. Biexponential signal attenuation analysis of diffusion-weighted imaging of breast. Magn Reson Med Sci 2010; 9: 195-207.

[18] Koh DM, Collins DJ and Orton MR. Intravoxel incoherent motion in body diffusion-weighted MRI: reality and challenges. AJR Am J Roentgenol 2011; 196: 1351-1361.

[19] Nilsen LB, Fangberget A, Geier O and Seierstad T. Quantitative analysis of diffusion-weighted magnetic resonance imaging in malignant breast lesions using different b value combinations. Eur Radiol 2013; 23: 1027-1033.

[20] Eiada R, Chong J, Kulkarni S, Goldberg F and Muradali D. Papillary lesions of the breast: MRI, ultrasound, and mammographic appearances. AJR Am J Roentgenol 2012; 198: 264-271.

[21] Jagmohan P, Pool FJ, Putti TC and Wong J. Papillary lesions of the breast: imaging findings and diagnostic challenges. Diagn Interv Radiol 2013; 19: 471-478.

[22] Lee HJ, Rha SY, Chung YE, Shim HS, Kim YJ, Hur J, Hong YJ and Choi BW. Tumor perfusion-related parameter of diffusion-weighted magnetic resonance imaging: correlation with histological microvessel density. Magn Reson Med 2014; 71: 1554-1558.

[23] Hatakenaka M, Soeda H, Yabuuchi H, Matsuo Y, Kamitani T, Oda Y, Tsuneyoshi M and Honda H. Apparent diffusion coefficients of breast tumors: clinical application. Magn Reson Med Sci 2008; 7: 23-29.

[24] Yoshikawa MI, Ohsumi S, Sugata S, Kataoka M, Takashima S, Mochizuki T, Ikura H and Imai

Y. Relation between cancer cellularity and apparent diffusion coefficient values using diffusion-weighted magnetic resonance imaging in breast cancer. Radiat Med 2008; 26: 222-226.

[25] Rahbar H, Partridge SC, Demartini WB, Gutierrez RL, Allison KH, Peacock S and Lehman CD. In vivo assessment of ductal carcinoma in situ grade: a model incorporating dynamic contrast-enhanced and diffusion-weighted breast MR imaging parameters. Radiology 2012; 263: 374-382.

[26] Andreou A, Koh DM, Collins DJ, Blackledge M, Wallace T, Leach MO and Orton MR. Measurement reproducibility of perfusion fraction and pseudodiffusion coefficient derived by intravoxel incoherent motion diffusion-weighted MR imaging in normal liver and metastases. Eur Radiol 2013; 23: 428-434.